Available online at www.sciencedirect.com
ScienceDirect
Trans. Nonferrous Met. Soc. China 34(2024) 618−628
Transactions of Nonferrous Metals Society of China
www.tnmsc.cn

Tribological properties of Ni-based composite coatings with addition of Ag@Ni core−shell particles over multiple thermal cycles

Nai-ru HE[1,2], Zi-wen FANG[1], Jun-hong JIA[1], Jie YANG[1], Wei CHEN[1], Hua XIN[1]

1. College of Mechanical and Electrical Engineering, Shaanxi University of Science &Technology, Xi'an 710021, China;
2. State Key Laboratory of Solid Lubrication, Lanzhou Institute of Chemical Physics, Chinese Academy of Sciences, Lanzhou 730000, China

Received 30 August 2022; accepted 1 December 2022

Abstract: In order to inhibit the diffusion of Ag, Ag@Ni core−shell structure particles were prepared by the electroless plating, and then the NiCrAlY−Mo−Ag@Ni coatings were prepared by atmospheric plasma spraying. The effects of core−shell structure design on the mechanical and tribological properties of the coatings over multiple thermal cycles were researched in detail. The results show that the core−shell structure design of Ag could enhance the interfacial bonding strength between Ag and NiCrAlY by the Ni-coated layer, and then improve the hardness of the coating obviously. The Ni-coated layer inhibits the diffusion and dissipation of Ag effectively in the friction process at high temperatures. The friction coefficient and wear rate of the NiCrAlY−Mo−Ag@Ni coating tested at 800 °C are only about 0.25 and 1×10^{-5} mm^3/(N·m), respectively, which are obviously lower than those of the NiCrAlY−Mo−Ag coating. Meanwhile, the core−shell structure design of Ag endows the coating with excellent self-lubricating and wear resistance over multiple thermal cycles.

Key words: core−shell structure; Ag@Ni; Ni-based composite coating; tribological properties; multiple thermal cycles

1 Introduction

With the rapid development of high-tech industries, higher requirements have been placed on the operation stability and reliability of the key moving components over a wide temperature range. The design of the solid self-lubricating materials operated over a wide temperature range has attracted considerable attention in the field of tribology [1−4]. Due to the low shear strength, the soft metals (Ag, Au, Pb, Cu, etc.) have been widely used as lubricants doping in the solid self-lubricating materials to improve the tribological properties over a wide temperature range [5−7].

At the end of the 20th century, DELLACORTE [8] and SLINEY et al [9] developed the adaptive Ni-based high temperature solid-lubricating composite coatings (PS family). With addition of Ag and BaF_2/CaF_2 eutectic, the PS family coatings have excellent tribological properties over a wide temperature range, in which PS200 and PS304 have been widely used for moving parts in aviation and aerospace engineering. The formation of the continuous Ag films on worn surface could provide lubrication at low and moderate temperatures, while the softened BaF_2/CaF_2 eutectic could provide lubrication at high temperatures. Moreover, for the materials with Ag and Tm (Tm=Mo, V, Ta, Nb) addition, $AgTm_xO_y$ generated by high temperature tribochemical reaction could also provide lubricating at high temperatures [10,11]. Soft metals, such as Ag, have been widely used in the self-lubricating materials over a wide temperature

Corresponding author: Jun-hong JIA, Tel: +86-13609383282, E-mail: jhjiasust@163.com
DOI: 10.1016/S1003-6326(23)66422-2

range. However, reports indicated that soft metals (Ag, Cu, Au, etc.) have a large diffusion coefficient at high temperatures and dissipate quickly during the friction process [11−13]. For instance, MULLIGAN et al [12] investigated the diffusion of Ag in the Cr−Ag films deposited by magnetron sputtering. They concluded that the diffusion of Ag is related to the temperatures of film deposition and friction test. Moreover, MURATORE et al [13] reported the diffusion mechanisms of Ag in the YSZ−Ag−Mo nanocomposite coatings. Ag was constantly consumed under the synergetic effects of heat and load during high-temperature friction test. And then, it was difficult to maintain the formation of lubricating film on the worn surface of the coating after being tested at high temperatures. More seriously, the depletion of Ag led to an increase of defects in the materials, such as pores, and then resulted in a sharp decrease of the mechanical properties.

To solve the rapid dissipation of Ag, MURATORE et al [13] fabricated the YSZ−Ag−Mo/TiN adaptive composite coatings. The TiN barrier layer could limit the dissipation of Ag at high temperatures by only allowing Ag diffusion through the pores in the TiN barrier layer. The addition of TiN barrier layers could improve the multicycle lubrication life of the composite coatings. In addition, the core−shell structure has been widely used on drug release [14,15]. For the solid lubrication materials, the core−shell structure design of the solid lubricants could improve the mechanical and tribological properties markedly [16−18]. Therefore, it could be deduced that the core−shell structure design of Ag could also improve the service life of the self-lubrication materials operated over a wide temperature range by limiting the diffusion and dissipation of Ag at high temperatures. However, there are few studies on the core−shell structure design of solid lubricants to improve the service life and tribological properties at elevated temperatures.

In this work, Ag@Ni core−shell structure particles were prepared to improve the service life and tribological properties of the Ni-based composite coatings. The microstructure evolution, mechanical and tribological properties of the composite coatings over multiple thermal cycles were studied in detail. The effects of Ag@Ni core−shell structure particles on the wear mechanisms and service life of the Ni-based composite coatings were revealed.

2 Experimental

2.1 Fabrication of Ni-based composite coatings

The Ag@Ni (Ag 40 wt.% and Ni 60 wt.%) core−shell structure particles were prepared by the electroless plating [19,20], in which nickel sulfate, sodium hypophosphite, sodium citrate, and Ag particles were used as raw materials. The sizes of agglomerates for Ag@Ni core−shell structure particles were 40−70 μm. The NiCrAlY powders (main composition: Ni Bal., Cr 21.85 wt.%, Al 9.56 wt.%, and Y 0.95 wt.%) were provided by Oerlikon Metco. Ag and Mo powders were obtained from Zhong Hang Zhong Mai Metal Material, China. And the sizes of NiCrAlY, Ag and Mo powders were 30−50, 40−60 and 40−60 μm, respectively. The feedstock powders were mixed in a three-dimensional mixing apparatus (M10, Grinder, China). Before spraying, the substrates were sandblasted and ultrasonically cleaned with alcohol. A thin NiCrAlY adhesion layer was prepared on the Inconel 718 alloys (*d*25 mm, 8 mm in thickness, main composition: Ni 51.2 wt.%, Cr 19.7 wt.%, Mo 3.2 wt.%, Al 0.4 wt.%, Nb 5.4 wt.%, Ti 1.3 wt.% and Fe 18.8 wt.%) to enhance the bonding strength, and then the NiCrAlY−Mo−Ag@Ni and NiCrAlY−Mo−Ag (for comparison) coatings were prepared by the atmospheric plasma spraying (APS−3000A). The proportion of Ag@Ni was determined by Ag content. The compositions of the composite coatings and the spraying parameters are shown in Table 1 and Table 2, respectively.

Table 1 Compositions of powders for composite coatings

Sample	Composition/wt.%			
	NiCrAlY	Mo	Ag	Ag@Ni
NM−Ag	80	10	10	0
NM−Ag@Ni	65	10	0	25

Table 2 Plasma spraying parameters of composite coatings

Parameter	Value
Current/A	550
Voltage/V	55
Ar flow rate/(L·min^{-1})	40
H_2 flow rate/(L·min^{-1})	6
Power feed rate/(g·min^{-1})	45
Spraying distance/mm	100

2.2 Mechanical properties tests

The microhardness of the composite coatings was measured using a Vickers hardness tester (HV−1000A) with a load of 200 g and a dwelling time of 10 s. Ten points were selected randomly from each sample to obtain the average hardness values. The bonding strength of the composite coatings was measured by the ASTM C633 standard test.

2.3 Tribological properties tests

Before the tribological properties tests, the composite coatings were polished to a roughness of about 40 nm and then cleaned by using ultra-sonication with acetone and alcohol. The tribological properties tests of the composite coatings were performed on a high-temperature ball-on-disk tribometer (HT−1000). The Si_3N_4 ball (d6 mm; hardness HV 1700) was used as the counterpart. The tribological properties tests of the composite coatings were implemented with a sliding speed of 0.3 m/s, a load of 5 N, and a test time of 60 min. The wear track radius was set to be 5 mm. The test temperatures were set to be RT (room temperature), 400, 600, and 800 °C. Each test was repeated three times. The multicycle friction tests of the composite coatings were implemented with the same parameters as a friction test at 800 °C. The wear volume was obtained by the Micro XAM 3D non-contact surface mapping profiler, and the wear rates (W, mm^3/(N·m)) of the composite coatings were calculated according to $W=V/(PL)$, where V is the wear volume (mm^3), P is the applied load (N), and L is the sliding distance (m).

2.4 Characterization of Ni-based composite coatings

The phase structure of the composite coatings was characterized by X-ray diffraction (XRD, Smart-Lab, Rigaku Corporation) with a scanning step of 10 (°)/min from 30° to 90° at 40 kV. The morphologies of the powders and the composite coatings were observed by scanning electron microscopy (SEM, TESCAN-MIRA3). The morphologies of the worn surfaces and the elemental compositions were analyzed by SEM coupled with an EDS detector. The phase compositions of the worn surfaces were detected by Raman spectrometry (Renishaw-inVia, UK).

3 Results and discussion

3.1 Microstructure and mechanical properties

Figure 1(a) displays the schematic diagram of the synthesis procedure of the Ag@Ni core−shell structure particles. Firstly, the Ag particles were activated under acidic conditions for 30 min to obtain greater surface activity. Then, the activated Ag powders were added to the alkaline electroless plating solution, which contained nickel sulfate, sodium hypophosphite, sodium citrate, and ammonia water for electroless plating in a 75 °C water bath for 2 h. The structure and morphology of the synthesized Ag@Ni particles are shown in Figs. 1(b) and (c), respectively. The XRD and SEM results demonstrate that Ag@Ni core−shell structure particles have great encapsulation and phase stability.

As shown in Table 3, the microhardness of the NM−Ag coating is about HV 251, while that of the NM−Ag@Ni coating is about HV 300. Compared with the NM−Ag coating, the coating with Ag@Ni addition possesses a much higher hardness, which means that the coated Ni layer enhances the interfacial bonding strength between Ag and NiCrAlY. Meanwhile, due to the same adhesion layer, the composite coatings have a similar binding strength.

The XRD patterns of the composite coating are shown in Fig. 2. The results show that the composite coatings consist of the Ni_3Al (γ' phase), Ag, and Mo phases, indicating that the feedstock powders are sprayed without experiencing any oxidation or decomposition under the experimental spraying parameters. Cross-sectional morphologies of the composite coatings are shown in Fig. 3. The composite coatings present a dense layered structure, which could be resulted from the flattening behavior of the thermally sprayed metallic materials. Moreover, Ag@Ni, Ag and Mo particles are distributed in the coatings uniformly.

3.2 Tribological behaviors

3.2.1 Tribological properties from RT to 800 °C

The average friction coefficients and the wear rates of the composite coatings are given in Fig. 4(a). The friction coefficients constantly decrease with increasing the temperature, while the

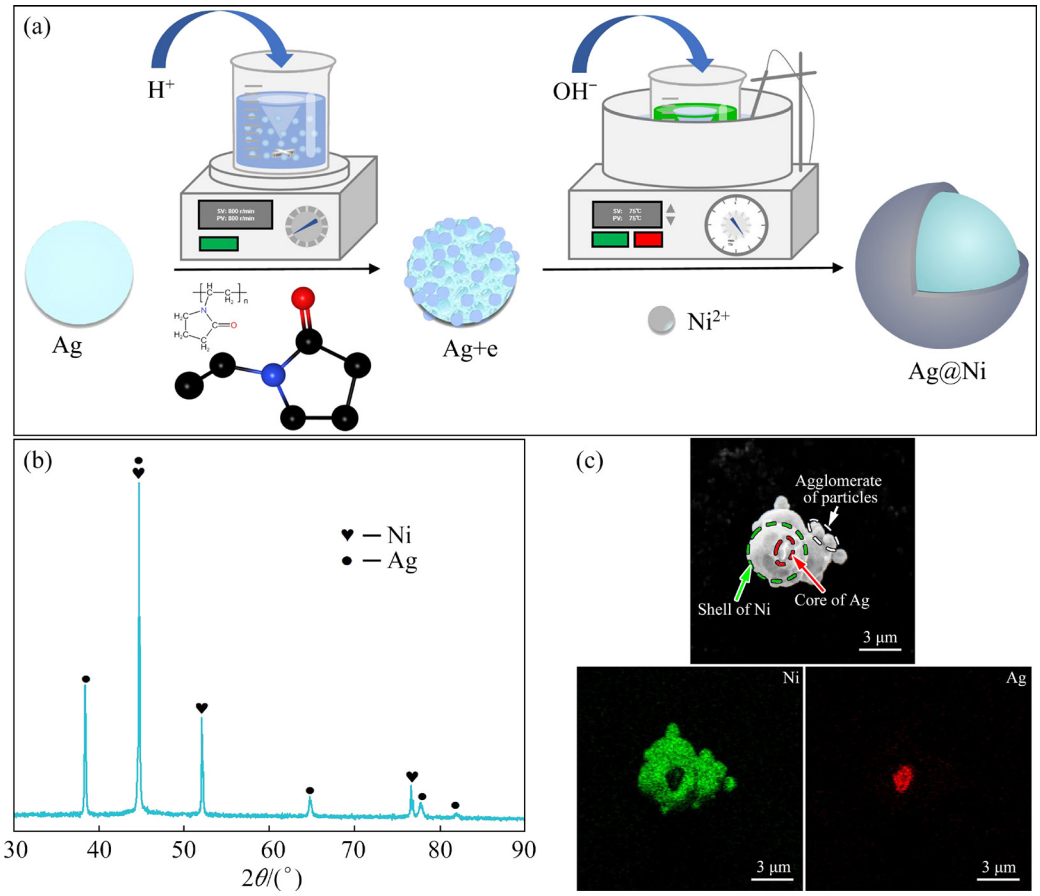

Fig. 1 Preparation and characterization of Ag@Ni particles: (a) Schematic diagram of electroless plating preparation; (b) XRD pattern; (c) SEM image and EDS mappings

Table 3 Mechanical properties of composite coatings

Sample	Bonding strength/ MPa	Microhardness (HV)	
		Original	After 5 thermal cycles test
NM−Ag	43±2.2	251.0±14.5	234.9±9.1
NM−Ag@Ni	44±2.6	300.0±19.3	298.5±16.1

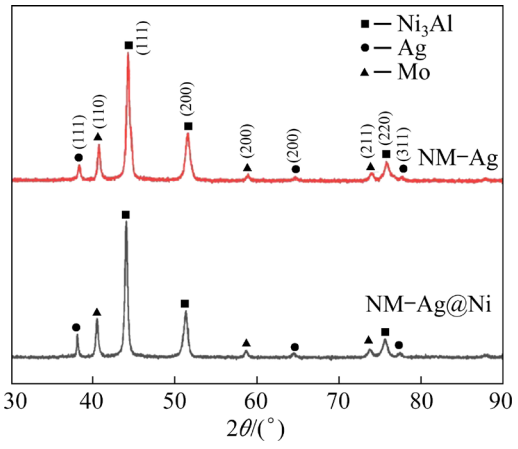

Fig. 2 XRD patterns of composite coatings

wear rates increase sharply at 400 °C and then decrease with further increasing the temperature. At RT, the friction coefficient of the NM−Ag@Ni coating is slightly higher than that of the NM−Ag coating, which means that the coated Ni layer hinders the formation of Ag lubricating film on the worn surface. Meanwhile, the wear rate of the NM−Ag@Ni coating is higher than that of the NM−Ag coating. With increasing the testing temperature, the shear strength of Ag decreases, which leads to the decrease of the friction coefficients. At 400 and 600 °C, the NM−Ag and NM−Ag@Ni coatings have similar friction coefficients and wear rates. The lowest friction coefficients and wear rates of the composite coatings were all obtained at 800 °C. And the friction coefficient of the NM−Ag@Ni coating is lower than that of the NM−Ag coating tested at 800 °C, meanwhile the wear rate of the NM−Ag@Ni coating is significantly lower than that of the NM−Ag coating. To further analyze the effects of the core−shell structure design of Ag on

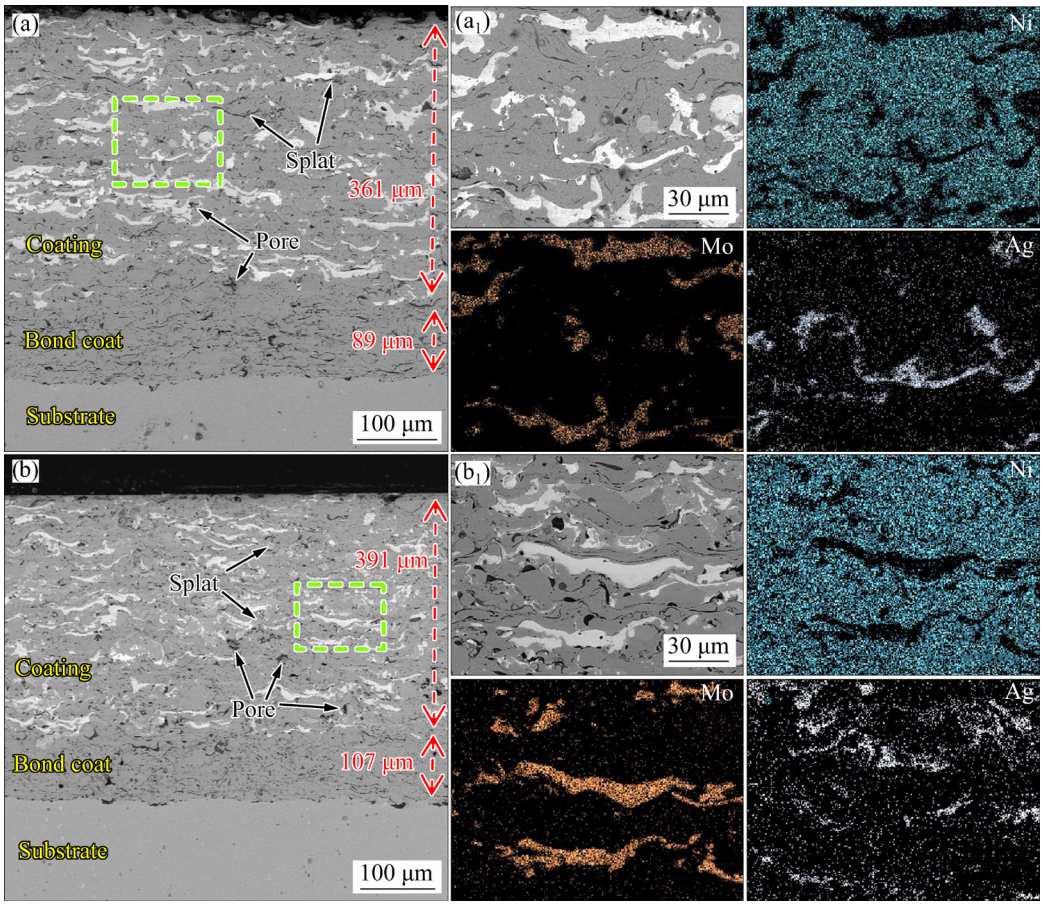

Fig. 3 Cross-sectional morphologies (a, b) and EDS analysis results (a_1, b_1) of composite coatings: (a, a_1) NM−Ag; (b, b_1) NM−Ag@Ni

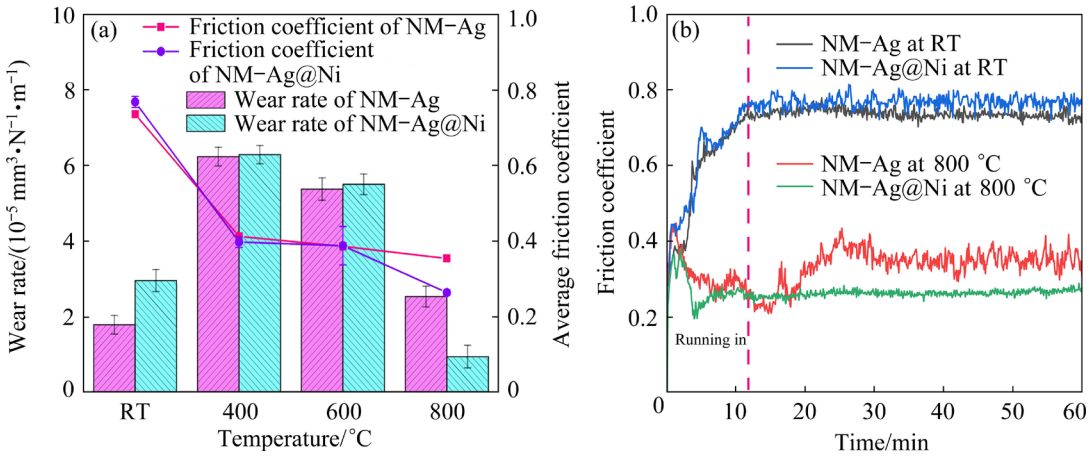

Fig. 4 Average friction coefficients and wear rates of composite coatings (a), and friction curves of composite coatings tested at RT and 800 ℃ (b)

the friction process, the friction curves of the composite coatings are given in Fig. 4(b). At RT, the friction coefficients of the NM−Ag and NM−Ag@Ni coatings stabilize at 0.75 and 0.78, respectively, after a long running-in period of about 12 min. It is worth noting that the friction curve of NM−Ag shows greater volatility at 800 ℃, and the average friction coefficient is about 0.36. In contrast, a stable friction curve and a lower friction coefficient of about 0.25 of the NM−Ag@Ni coating is obtained.

To analyze the effects of the core−shell

structure design of Ag on the wear mechanisms of the composite coatings, the worn surface morphologies at the RT and 800 ℃ are shown in Fig. 5. At 400 and 600 ℃, the composite coatings possess similar friction coefficients and wear rates, and the wear mechanisms were researched [11,13]. Therefore, the wear mechanisms of the composite coatings tested in the medium temperature range are not discussed in this work. As shown in Figs. 5(a) and (b), the worn surfaces of the composite coatings are all covered with evident delamination. Although a small amount of Ag addition cannot form a continuous lubricating film on the worn surface and the coating possesses a lower hardness, the friction coefficient and wear rate of the NM−Ag coating are all lower than those of the NM−Ag@Ni coating at RT. The core−shell structure design of Ag makes it difficult for Ag to lubricate effectively at RT. In addition, surface fatigue spalling of NiCrAlY occurs on the composite coating surface under the action of cyclic stress caused by the counterpart. When the test temperature reaches 800 °C, an oxide layer can be found on the worn surfaces of the NM−Ag coating. The EDS mappings in Fig. 6(a) indicate an obvious oxidation phenomenon without element enrichment on the worn surface. Moreover, Ag content on the worn surface increases to 18.1 wt.% compared with the original coating.

The Raman spectra of the worn surfaces of the composite coatings after being tested at 800 ℃ are exhibited in Fig. 7. As shown in Fig. 7(a), Ag_2MoO_4, $Ag_2Mo_4O_{13}$, and $NiMoO_4$ were detected from the worn surface of the NM−Ag coating. Researchers in Refs. [21,22] found that lots of double-metal-oxides, such as Ag_2MoO_4, $Ag_2Mo_4O_{13}$, and $NiMoO_4$, have a low melting temperature and a layered structure with easily breakable bonds, which endow the materials with a low friction coefficient and wear rate at high temperatures. For the NM−Ag@Ni coating, the EDS mappings of the worn surface in Fig. 6(b) show an obvious Ni and Ag enrichment in the tribo-layer on the worn surface. Similarly, the large amount of O indicates the oxidation of the coating surface. Different from the phase composition of the NM−Ag coating, NiO, which has an excellent self-lubricating property, was also detected from the Raman spectrum of the NM−Ag@Ni coating. The synergistic lubrication of NiO and the double-metal-oxides demonstrates better lubrication and wear resistance of the NM−Ag@Ni coating compared with the NM−Ag coating.

3.2.2 Tribological properties over multiple thermal cycles

To investigate the effects of the core−shell structure design of Ag on the lubrication life of the coating over the wide temperature range, the multicycle friction tests at 800 °C were conducted. The friction curves of the composite coatings over multiple thermal cycles are given in Fig. 8. The friction coefficients of the NM−Ag coating fluctuate significantly in the sliding process, and the average friction coefficients of the NM−Ag coating are all higher than 0.25 in 5 cycles test. For the NM−Ag@Ni coating, the friction curves are very stable, and the average friction coefficients are only about 0.2 in 5 cycles test. The wear rates of the composite coatings after being tested at 800 ℃ over multiple thermal cycles are shown in Fig. 9. It can be realized that the wear rates of the NM−Ag coating increase sharply with increasing the testing cycles. Significantly, with the testing cycles increasing, there is no apparent change of the wear rate of the NM−Ag@Ni coating. After 5 thermal cycles test, the wear rate of the NM−Ag@Ni coating is only about 1.5×10^{-5} $mm^3/(N\cdot m)$, which is

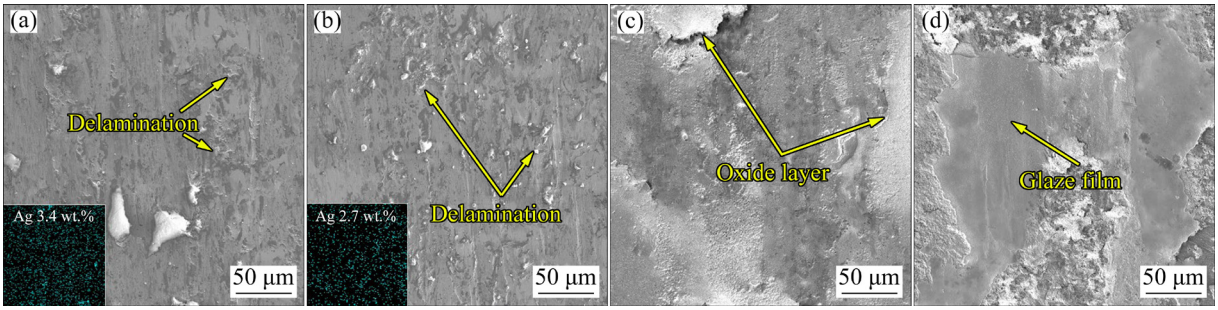

Fig. 5 Worn surface morphologies of composite coatings: (a) NM−Ag at RT; (b) NM−Ag@Ni at RT; (c) NM−Ag at 800 ℃; (d) NM−Ag@Ni at 800 ℃

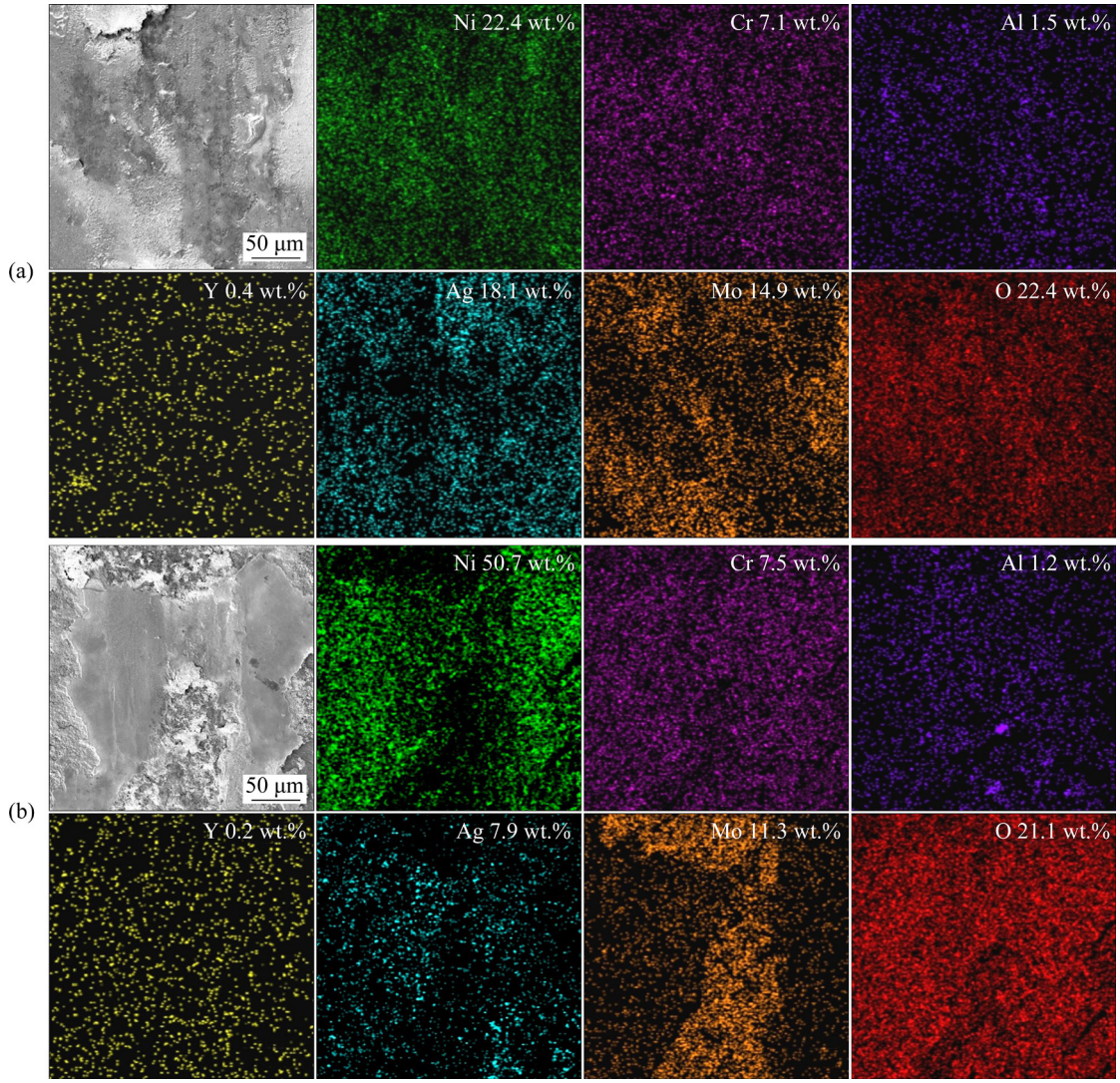

Fig. 6 Element mappings of worn surfaces of composite coatings at 800 °C: (a) NM−Ag; (b) NM−Ag@Ni

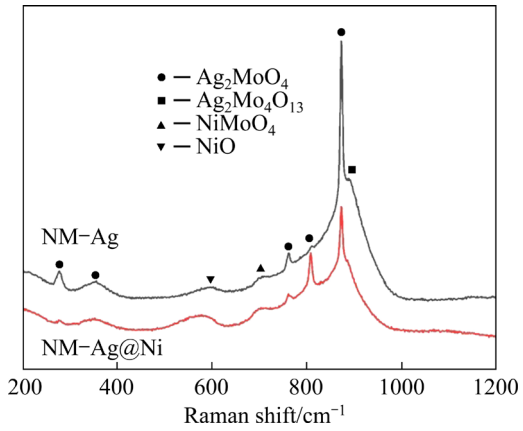

Fig. 7 Raman spectra of worn surfaces of composite coatings at 800 °C

markedly lower than that of the NM−Ag coating (10.5×10^{-5} mm^3/(N·m)). The ratio of W_{NM-Ag} (wear rate of NM−Ag coating) to $W_{NM-Ag@Ni}$ (wear rate of NM−Ag@Ni coating) is calculated and given in Fig. 9. The ratios of the wear rates remain at 2.7 in Cycles 1 and 2, while the ratios increase sharply in the subsequent thermal cycles. Compared to the traditional Ag addition, Ag@Ni addition could improve the wear-resistant life of the coating significantly.

Figure 10 presents the worn surface morphologies of the composite coatings after being tested at 800 °C over multiple thermal cycles. In the first four cycles, the NM−Ag coating has similar worn surface morphologies. According to the wear mechanisms mentioned above, oxidative wear occupied in the friction process of the NM−Ag coating. It can be seen from Fig. 10(d) that a tribo-film is formed on the worn surface of the NM−Ag coating after 5 thermal cycles test. Furthermore, there is always a tribo-layer on the worn

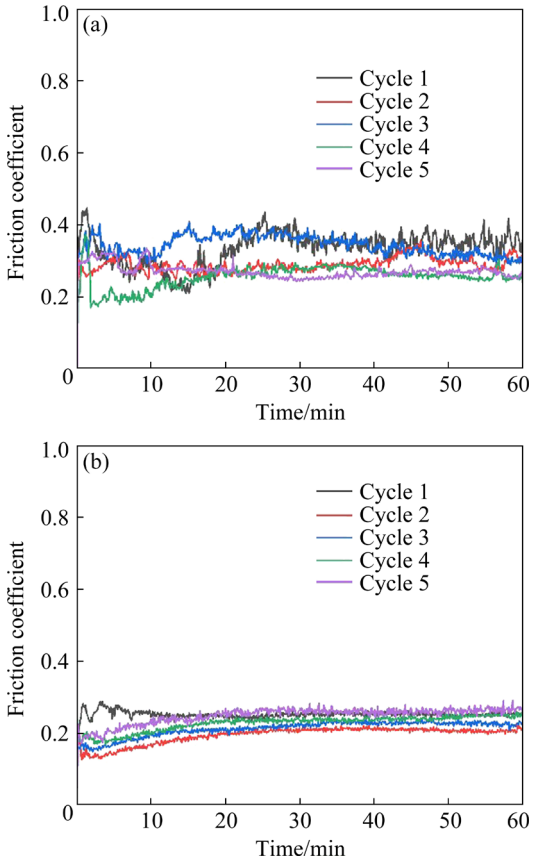

Fig. 8 Friction curves of composite coatings at 800 ℃ over multiple thermal cycles: (a) NM−Ag; (b) NM−Ag@Ni

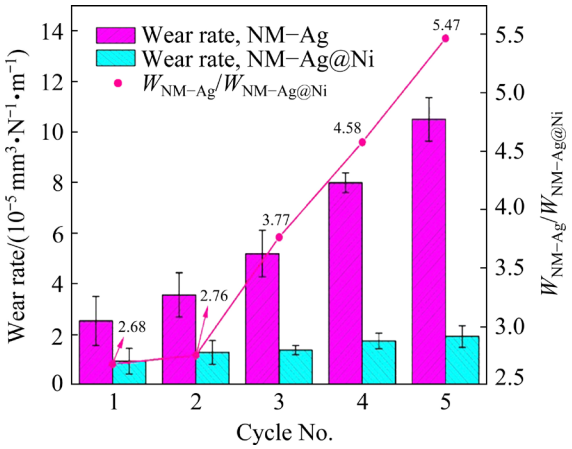

Fig. 9 Wear rates and ratio of W_{NM-Ag} to $W_{NM-Ag@Ni}$ of composite coatings at 800 ℃ over multiple thermal cycles

surface of the NM−Ag@Ni coating in the cycle test. In order to research the evolution of the phase composition on the worn surface, the Raman scattering was carried out and given in Fig. 11. As shown in Fig. 11(a), Raman spectrum of the tribo-film on the NM−Ag coating after 5 thermal cycles test shows obvious $NiMoO_4$ and Ag_2MoO_4 peaks, as well as a weak MoO_3 peak. However, as shown in Fig. 11(b), an evident peak of Ag_2MoO_4 and a weak peak of NiO appear in the spectrum of the tribo-layer of the NM−Ag@Ni coating after 5 cycles test. Compared with the phase composition shown in Fig. 7, it is difficult to form silver molybdate continuingly on the worn surface of the NM−Ag coating with increasing the testing cycles. Instead of Ag_2MoO_4, $NiMoO_4$ is formed by high temperature tribo-chemical reaction of NiO and MoO_3. By the core−shell structure design of Ag, Ag_2MoO_4 is formed continuously on the worn

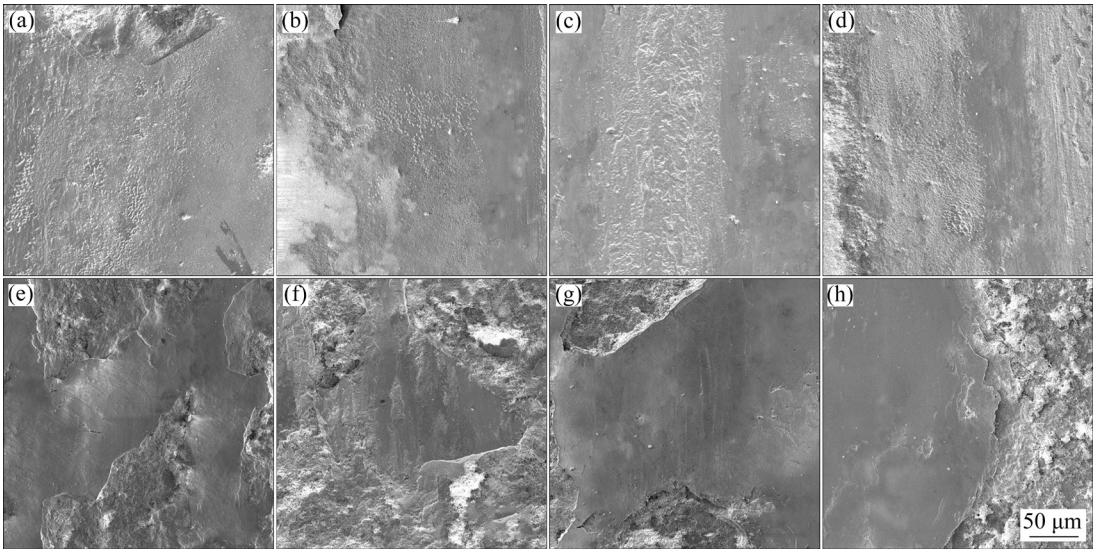

Fig. 10 Worn surface morphologies of NM−Ag (a−d) and NM−Ag@Ni (e−h) coatings at Cycles 2−5, respectively

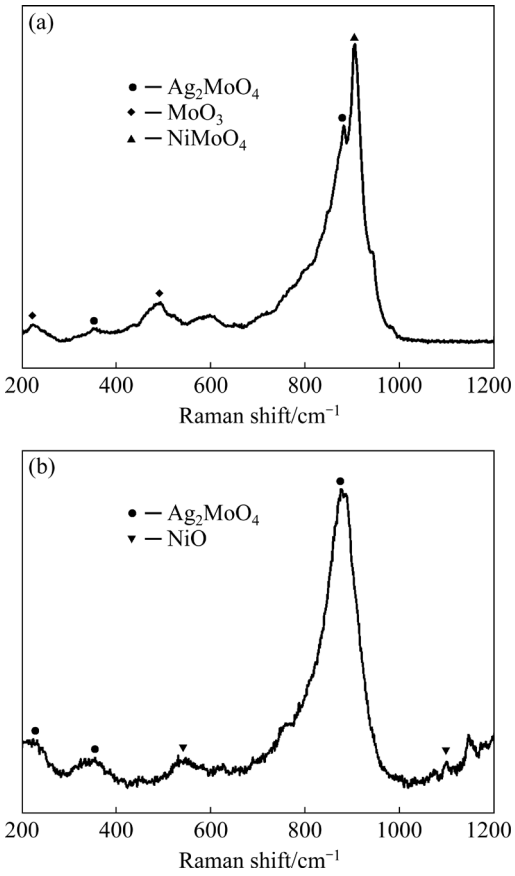

Fig. 11 Raman spectra of worn surfaces of composite coatings after 5 cycles test: (a) NM−Ag; (b) NM−Ag@Ni

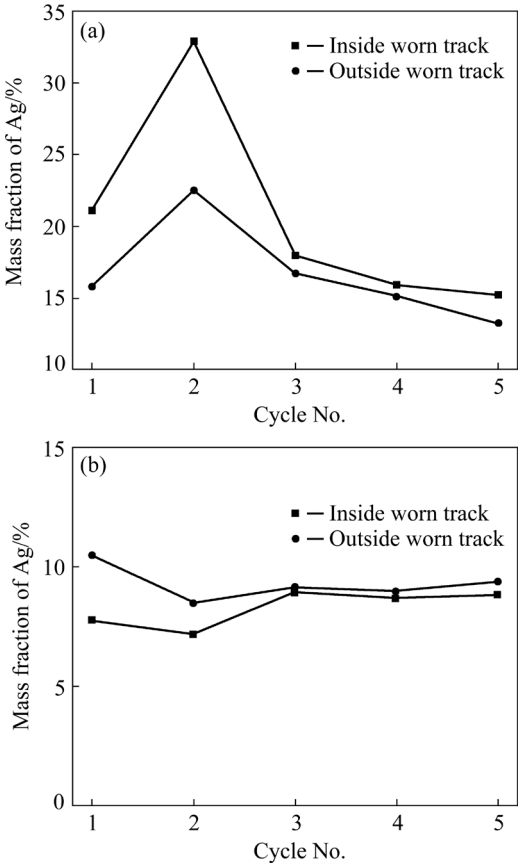

Fig. 12 Mass fractions of Ag on worn surfaces of composite coatings at 800 ℃ over multiple thermal cycles: (a) NM−Ag; (b) NM−Ag@Ni

surface in the process of high temperature test, which could also correspond to the stable friction curves, low friction coefficients and wear rates of the NM−Ag@Ni coating in the cycle test.

To analyze the chemical composition of the composite coatings after multicycle friction tests at 800 ℃, the mass fractions of Ag on the surfaces of the composite coatings after multicycle friction tests are shown in Fig. 12. For the NM−Ag coating, with increasing the testing cycles, the mass fractions of Ag both inside and outside of the worn track increase firstly, and then decrease sharply due to the combination of multicycle stress and heat [20,22]. The rapid dissipation of Ag could be responsible for the domained $NiMoO_4$ on the worn surface. For the NM−Ag@Ni coating, it is worth noting that the mass fractions of Ag are stable both inside and outside of the worn track. Meanwhile, the mass fraction of Ag of the coating after 5 thermal cycles test is similar to that of the original coating. Although the Ag content decreases significantly after the cycles test, Ag content on the surface of the NM−Ag coating is higher than that of the NM−Ag@Ni coating and the original coating. For this reason, Ag contents on the cross-section of the composite coatings are given in Fig. 13. Ag content in the NM−Ag coating shows a pronounced downtrend, and Ag content in the stress-affected area of the coating after 5 cycles test is only about 2.3 wt.%, which is obviously lower than that of the original coating. The Vickers hardness tested on the cross-section of the composite coatings is also listed in Table 3. The average hardness of the NM−Ag coating after 5 cycles test is significantly lower than that of the original coating. The loss of Ag results in the generation of internal defects (cracks and pores) in the NM−Ag coating, therefore decreasing the mechanical properties. Compared with that in the NM−Ag coating, the Ag content in the NM−Ag@Ni coating maintains a stable level, and the hardness remains at HV 298.5 after 5 cycles test, which are close to those of the original coating. That is to say, the core−shell structure design of Ag could limit the diffusion effectively and maintain

the mechanical properties of the coating in the friction test at high temperatures over multiple thermal cycles.

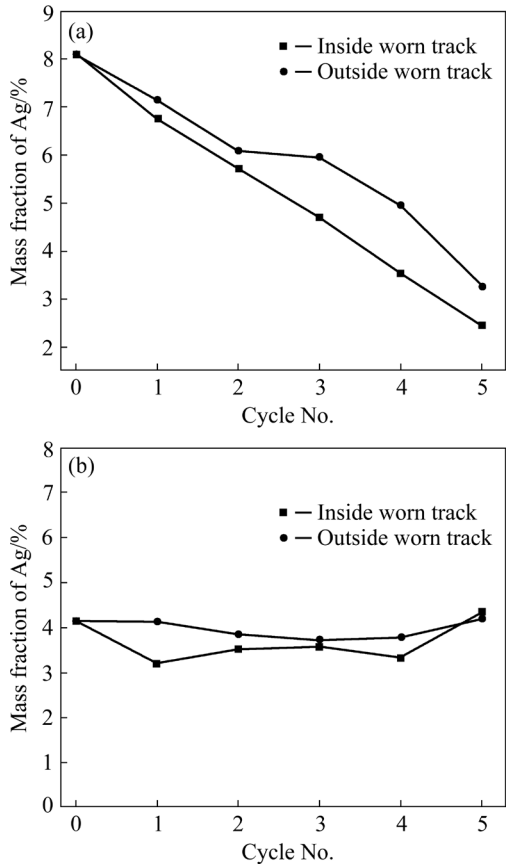

Fig. 13 Mass fractions of Ag on cross-section of composite coatings at 800 ℃ over multiple thermal cycles: (a) NM−Ag; (b) NM−Ag@Ni

4 Conclusions

(1) The coated Ni layer could improve the microhardness of the composite coating by enhancing the interfacial bonding strength between Ag and NiCrAlY. However, the core−shell structure design of Ag makes it difficult for Ag to effectively lubricate at low temperatures.

(2) At 800 ℃, a stable friction curve with a lower average friction coefficient of about 0.25 is obtained from the NM−Ag@Ni coating. Meanwhile, the wear rate of the NM−Ag@Ni coating is only about 1×10^{-5} mm^3/(N·m), which is significantly lower than that of the NM−Ag coating.

(3) In the cycles test at 800 ℃, the NM−Ag@Ni coating always shows stable friction curves and wear rates, while the wear rates of the NM−Ag coating increase sharply due to the rapid dissipation of Ag.

(4) The core−shell structure design inhibits the diffusion and dissipation of Ag significantly during the friction test at high temperatures. After 5 cycles test, the defects caused by Ag diffusion in the NM−Ag coating decrease the microhardness obviously, while the NM−Ag@Ni coating retains a similar hardness to that of the original coating.

CRediT authorship contribution statement

Nai-ru HE: Resources, Project administration, Conceptualization, Funding acquisition, Investigation, Data curation, Writing − Review & editing; **Zi-wen FANG:** Investigation, Data curation, Visualization, Writing − Original draft & methodology; **Jun-hong JIA:** Conceptualization, Writing − Review & editing, Project administration; **Jie YANG:** Investigation, Visualization, Data curation; **Wei CHEN:** Investigation, Writing − Review & editing; **Hua XIN:** Writing − Review & editing.

Declaration of competing interest

The authors declare that they have no known competing financial interests or personal relationships that could have appeared to influence the work reported in this paper.

Acknowledgments

The authors are grateful to the National Natural Science Foundation of China (No. 51905325), and the China Postdoctoral Science Foundation (No. 2019M653525).

References

[1] CHEN Jian-min, LU Xiao-wei, LI Hong-xuan, ZHOU Hui-di. Progress of solid self-lubricating coating over a wide range of temperature [J]. Tribology, 2014, 34(5): 592−600. (in Chinese)

[2] ZHU Sheng-yu, CHENG Jun, QIAO Zhu-hui, YANG Jun. High temperature solid-lubricating materials: A review [J]. Tribology International, 2019, 133: 206−223.

[3] ZHAO Yong-qiang, MU Yong-tao, LIU Ming. Mechanical properties and friction-wear characteristics of VN/Ag multilayer coatings with heterogeneous and transition interfaces [J]. Transactions of Nonferrous Metals Society of China, 2020, 30: 472−483.

[4] VOEVODIN A A, MURATORE C, AOUADI S M. Hard coatings with high temperature adaptive lubrication and contact thermal management: Review [J]. Surface and Coatings Technology, 2014, 257: 247−265.

[5] WU Ji-si, LI Jing-fu, ZHANG Lei, QIAN Zhi-yuan. Effects of environment on dry sliding wear behavior of silver−copper based composites containing tungsten disulfide [J]. Transactions of Nonferrous Metals Society of China, 2017, 27: 2202−2213.

[6] HE Peng-fei, WANG Hai-dou, MA Guo-zheng, YONG Qing-song, CHEN Shu-ying, XU Bin-shi. Research progress of high-temperature tribological properties of silver-containing hard coatings [J]. The Chinese Journal of Nonferrous Metals, 2015, 25(11): 2962−2974. (in Chinese)
[7] XU Xing, SUN Jian-fang, SU Feng-hua, LI Zhu-jun, CHEN Yan-jun, XU Zhi-biao. Microstructure and tribological performance of adaptive MoN−Ag nanocomposite coatings with various Ag contents [J]. Wear, 2022, 488/489: 204170.
[8] DELLACORTE C. The effect of counterface on the tribological performance of a high temperature solid lubricant composite from 25 to 650 °C [J]. Surface and Coatings Technology, 1996, 86/87: 486−492.
[9] SLINEY H E, LOOMIS W R, DELLACORTE C. Evaluation of PS 212 coatings under boundary lubrication conditions with an ester-based oil to 300 °C [J]. Surface and Coatings Technology, 1995, 76/77: 407−414.
[10] WANG Dan, CHEN Wen-yuan, SUN Qi-chun, WANG Long, ZHU Sheng-yu, CHENG Jun, YANG Jun. Tribological properties of Ni_3Al−Ni_3Nb−Ag self-lubricating alloys at a wide temperature range [J]. Wear, 2021, 480/481: 203933.
[11] HU J J, MURATORE C, VOEVODIN A A. Silver diffusion and high-temperature lubrication mechanisms of YSZ−Ag−Mo based nanocomposite coatings [J]. Composites Science and Technology, 2007, 67: 336−347.
[12] MULLIGAN C P, BLANCHET T A, GALL D. Control of lubricant transport by a CrN diffusion barrier layer during high-temperature sliding of a CrN−Ag composite coating [J]. Surface and Coatings Technology, 2010, 205: 1350−1355.
[13] MURATORE C, HU J J, VOEVODIN A A. Adaptive nanocomposite coatings with a titanium nitride diffusion barrier mask for high-temperature tribological applications [J]. Thin Solid Films, 2007, 515: 3638−3643.
[14] HORCAJADA P, CHALATI T, SERRE C, GILLET B, SEBRIE C, BAATI T, EUBANK J F, HEURTAUX D, CLAYETTE P, KREUZ C, CHANG J S. Porous metal-organic-framework nanoscale carriers as a potential platform for drug delivery and imaging [J]. Nature Materials, 2010, 9: 172−178.
[15] TZUR-BALTER A, SHATSBERG Z, BECKERMAN M, SEGAL E, ARTZI N. Mechanism of erosion of nanostructured porous silicon drug carriers in neoplastic tissues [J]. Nature Communications, 2015, 6: 6208.
[16] LIN Qi-lan, WANG Xun, CAI Meng, YAN Han, ZHAO Zhuang, FAN Xiao-qiang, ZHU Min-hao. Enhancement of Si_3N_4@MoS_2 core-shell structure on wear/corrosion resistance of epoxy resin/polyacrylate IPN composite coating [J]. Applied Surface Science, 2021, 568: 150938.
[17] HUANG Jian, LI Yong, JIA Xiao-hua, SONG Hao-jie. Preparation and tribological properties of core−shell Fe_3O_4@C microspheres [J]. Tribology International, 2019, 129: 427−435.
[18] YANG Ya-wen, WANG Hong-gang, REN Jun-fang, GAO Gui, CHEN Sheng-sheng, WANG Na, ZHAO Geng-rui, WANG Jin-qing. Core-shell polytetrafluoroethylene @ phenolic resin composites: Structure and tribological behaviors [J]. Tribology International, 2020, 144: 106092.
[19] HE Nai-ru, FANG Zi-wen, JIA Jun-hong, LIU Ning, YANG Jie. Preparation and characterization of core−shell Ag@Ni powder [J]. China Powder Science and Technology, 2022, 28(2): 99−105. (in Chinese)
[20] VYKOUKAL V, ZELENKA F, BURSIK J, KANA T, KROUPA A, PINKAS J. Thermal properties of Ag@Ni core−shell nanoparticles [J]. Calphad, 2020, 69: 101741.
[21] WANG Dan, TAN Hui, CHEN Wen-yuan, ZHU Sheng-yu, CHENG Jun, YANG Jun. Tribological behavior of Ni_3Al−Ag based self-lubricating alloy with Ag_2MoO_4 formed by high temperature tribo-chemical reaction [J]. Tribology International, 2021, 153: 106659.
[22] STONE D, LIU J, SINGH D P, MURATORE C, VOEVODIN S A, MISHRA S, REBHOLZ C, GE Q, AOUADI A M. Layered atomic structures of double oxides for low shear strength at high temperatures [J]. Scripta Materialia, 2010, 62: 735−738.

含 Ag@Ni 核壳结构粉体镍基复合涂层的多循环高温摩擦学性能

何乃如[1,2]，方子文[1]，贾均红[1]，杨 杰[1]，陈 威[1]，辛 骅[1]

1. 陕西科技大学 机电工程学院，西安 710021；
2. 中国科学院 兰州化学物理研究所 固体润滑国家重点实验室，兰州 730000

摘 要：为了抑制 Ag 的扩散，采用化学镀方法制备 Ag@Ni 核壳结构粉体，并利用大气等离子喷涂技术制备 NiCrAlY−Mo−Ag@Ni 涂层，详细研究核壳结构设计对涂层在高温循环工况下的力学及摩擦学性能的影响。研究结果表明：Ag 的核壳结构设计可以提高镍基涂层中 Ag 与 NiCrAlY 的界面结合强度，进而显著提高复合涂层的硬度。Ni 覆层有效地抑制了 Ag 在高温摩擦过程中的扩散与耗散。800 ℃时 NiCrAlY−Mo−Ag@Ni 涂层的摩擦因数仅为 0.25，磨损率仅为 1×10^{-5} $mm^3/(N\cdot m)$，显著低于 NiCrAlY−Mo−Ag 涂层。同时，Ag 的核壳结构设计使得涂层在高温多循环工况下始终保持良好的自润滑性和耐磨性。

关键词：核壳结构；Ag@Ni；Ni 基复合涂层；摩擦学性能；高温热循环

(Edited by Wei-ping CHEN)